PIBB 生物化学与生物物理进展
Progress in Biochemistry and Biophysics
2021,48(9):1052~1062
www.pibb.ac.cn

Crystal Structure of an O−acyltransfer Terminal Protein stDltD and Its Implications for dlt Operon−mediated D−alanylation of *S. thermophilus**

ZENG Qi[1,2], TIAN Li-Fei[1], LIU Yan-Ping[1], YAN Xiao-Xue[1]**, XU Wen-Qing[1,3]**

([1]*National Laboratory of Biomacromolecules, CAS Center for Excellence in Biomacromolecules, Institute of Biophysics, Chinese Academy of Sciences, Beijing* 100101, China;
[2]*College of Life Sciences, University of Chinese Academy of Sciences, Beijing* 100049, China;
[3]*Shanghai Institute for Advanced Immunochemical Studies and School of Life Science and Technology, ShanghaiTech University, Shanghai* 201210, China)

Abstract In bacteria, the acyl transmembrane modification of cell-surface polymers is a common feature to strengthen their pathogenic potential. The dlt operon-mediated D-alanylation of lipoteichoic acids (LTAs) is an important post-modification to adjust charge balance in Gram-positive bacteria. Four proteins of DltA/B/C/D were identified to be essential for LTA D-alanine incorporation. Though the process of D-alanine transfer by cytoplasmic DltA/DltC has been largely probed, transmembrane catalysis by MBOAT protein DltB and the terminal player DltD is yet to be defined. Here, the crystal structure of stDltD was determined from *S. thermophilus* at 2.94 Å resolution. On the basis of the structure comparison, DltD was considered as the terminal acyltransferase of the dlt operon, and it belonged to the SGNH-like family. An stDltD active center, including four blocks and a catalytic triad, conservatively exists in various Gram-positive pathogens. In addition, structural analysis showed that the stDltD catalytic center formed a strong positively charged groove docking with a glycerolphosphate molecule. Combined with previous reports, an updated working model was proposed for cross-membrane D-alanylation mediated by the dlt operon. The structural evidence provides more implications to clarify the biological function of stDltD and the process of transmembrane acyl modification.

Key words dlt operon, acyl transmembrane modification, LTA D-alanylation, SGNH-like family, crystal structure
DOI: 10.16476/j.pibb.2021.0020

Bacterial cell walls are structured by multiple biomolecular components (*e. g.* phospholipid, peptidoglycan, and proteins) with distinguishing features of long abundant amphiphilic polymer threading through the cell membrane layers, lipopolysaccharides in Gram-negative strains, and lipoteichoic acids (LTAs) and wall teichoic acid (WTA) in Gram-positive strains. Transmembrane modifications on those polymers alternate the cell-surface charge property, thus in turn modulate cellular growth and pathogenesis[1-4].

Membrane-anchored LTA and peptidoglycan-bound WTA share structural similarities comprising the disaccharide linkage unit and various lengths of polyol repeats (25 units for LTA and 40−60 units for WTA on average)[5-6]. By far, five types of LTA and four types of WTA were identified, among which type I LTA with glycerolphosphate (GroP) backbone widely exists in *B. subtilis*, *S. aureus*, *L. monocytogenes*, *E. faecalis*, *S. agalactiae*, and *S. pyogenes*[7-8]. The backbone hydroxyls were proven to be ubiquitously tailored with D-alanyl, glycosyl (glucose, GlcNAc, and mannose) [9-10], and phosphocholine on type IV LTA[11]. Depending on the

* This work was supported by grants from the Chinese Academy of Sciences Pilot Strategic Science and Technology Projects B grant (XDB37030302) and The National Natural Science Foundation of China (31629002), the National Laboratory of Biomacromolecules.
** Corresponding author.
YAN Xiao-Xue. Tel: 86-10-64888509, E-mail: snow@ibp.ac.cn
XU Wen-Qing. Tel: 86-10-64888509, E-mail: xuwq2@shanghaitech.edu.cn
Received: Janua y 19, 2021 Accepted: March 1, 2021

species, the specific contents ratio varies. For example, the modification landscape in *S. aureus* is 70% D-alanine, 15% GlcNAc, and 15% hydroxyls[12], while that in *B. subtilis* is 50% alanine, 20% GlcNAc, and 10% glucose[13]. Notably, D-alanine ester substitutions exhibit highly dynamic distributions compared with other modifications based on experimental evidence of non-enzymatic transacylation between lipophilic and endogenous hydrophilic LTAs[14], reversibility from membrane-associated D-alanyl back to D-alanyl-DltC[15]; re-esterification compensation for the loss of D-alanine ester under different pH values[16]; and sensibility to salt concentration, pH, and temperature[17].

The D-alanylations of LTA and WTA are accomplished by the dlt operon, highly functional related gene bundles encoding DltA/B/C/D. First, cytoplasmic DltA transfers D-alanine DltC to generate D-alanyl-DltC, which functions as a D-alanyl donor to promote the following reactions. Though the structural and functional information of two upstream proteins have been clarified, two membrane-associated proteins DltB and especially the terminal player DltD are largely unknown. A recent report showed that DltC forms a stable complex with DltB in its native (K_d=0.19 μmol/L) and D-alanyled state (K_d= 0.26 μmol/L)[18]. On the basis of structural evidence, researchers suggested that DltC sat at the cytoplasmic bottom tunnel of DltB, where DltC Ser35 and DltB His336 could be coordinated properly through the phosphopanteth eine (Ppant) group, thus driving the cross-membrane catalysis for LTA D-alanylation. However, how DltD is involved in this pathway remains unclear.

Here, the crystal structure of stDltD from *S. thermophilus* was resolved, and one internal core with high structural similarity to SGNH-like proteins was identified. The conserved catalytic triad was also defined. This study provides more implications to functionally characterize DltD during LTA D-alanylation and further evidence for transmembrane acyl modification.

1 Materials and Methods

1.1 Protein expression and purification

The extracellular domain of stDltD (28−422 aa) was cloned into pET-22b plasmid (Novagen) with a C-terminal His-tag, and was transformed into *E. coli* BL21(DE3) for protein expression. Cell cultures were induced with 0.4 mmol/L IPTG for 20 h at 18℃ when A_{600} reached roughly 0.8. The recombinant proteins were purified by sonication and three-step column chromatography using a Ni-affinity column, S fast flow column (GE Healthcare) and Superdex200 gel-filtration column (GE Healthcare). stDltD were concentrated to 12 g/L by ultrafiltration in 20 mmol/L Hepes pH 7.0, 100 mmol/L NaCl and 2 mmol/L DTT. The protein was stored at −80℃.

1.2 Crystallization and structure determination

Crystals of stDltD were obtained using the hanging-drop vapor diffusion technique at 20℃ with drops containing 1 μl of 3.3 g/L protein solution and 1 μl of reservoir solution (20% glycerol, 14% *w/v* PEG6000, 170 mmol/L $(NH_4)_2SO_4$). The crystals were straightly flash-frozen into liquid nitrogen. Data sets of stDltD crystals were collected at −163℃ on beamline BL19U1 at the Shanghai Synchrotron Radiation Facility (λ =1 Å). The diffraction images were indexed and integrated using HKL3000[19]. The structure of stDltD at resolution of 2.94 Å was solved by Molecular Replacement (MR) method using PHASER in the CCP4[20] with D-alanyl-lipoteichoic acid synthetase (PDB: 3BMA) from *Streptococcus pneumoniae* R6 as the initial model. The model was built and refined by PHENIX[21] and COOT[22]. After several rounds of refinement, the structure models reached an R_{work} and R_{free} of 21.65% and 23.58%. All structural images were drawn using PyMOL (http:// www. pymol. org/). Data collection statistics and crystallographic statistics are shown in Table 1.

1.3 Size−exclusion chromatography （SEC）

SEC was performed using a fast protein liquid chromatography system (GE Healthcare) on a Superdex200 HR 10/300 column at a flow rate of 0.5 ml/min. Sample was loaded onto the column equilibrated with 20 mmol/L Hepes pH 7.0, 100 mmol/L NaCl and 2 mmol/L DTT, and eluted with the same buffer. Protein elution was monitored by measuring the absorbance at 280 nm. Data analysis was conducted using UNICORN version 5.11 software program.

1.4 Thermofluor assay

Melting temperature of the wild type and triad 3M (S73A/D371A/D374A) of stDltD were measured using quantitative PCR machine Rotor-Gene 6600. Proteins were concentrated to 4 g/L, and then 18 μl

PBS were mixed with 1 μl protein and 1 μl SYPROTM ORANGE dye. The temperature gradient was set to a range from 20° C to 70℃ with 1℃/min increment.

1.5 Analytical ultracentrifugation （AUC）

Sedimentation velocity experiment was performed with a Beckman ProteomeLab XL-I analytical ultracentrifuge at 20℃ . Samples were prepared in a buffer containing 20 mmol/L Hepes pH 7.5, 150 mmol/L NaCl with 280 nm absorbance of 0.74. Data collection was performed at 50 000 r/min for 6 h. Finally, interference sedimentation coefficient distribution (C(M)) was calculated using software SEDFIT.

1.6 Data availability

Atomic coordinates and structure factors of stDltD have been deposited in the Protein Data Bank under accession numbers of 7DXM.

Table 1 X−ray Data collection and refinement statistics

		stDltD
Data collection	Space group	$P2_12_12_1$
	Cell dimensions	
	a, *b*, *c* (Å)	58.3, 109.9, 283.4
	α, *β*, *γ* (°)	90, 90, 90
	Wavelength/Å	1.000
	Resolution/Å	50.0-2.94 (2.94-3.01)
	R_{pim}/%	10.5 (57.3)
	I / σI	39.3 (3.0)
	CC1/2	0.984 (0.554)
	Completeness/%	99.2 (99.3)
	Redundancy	4.0 (3.7)
Refinement	Resolution/Å	39.99-2.94
	No. reflections	39 547
	R_{work} / R_{free}	21.65/23.58
	No. atoms	12 785
	Average B factor/Å^2	
	Protein	61.15
	SO_4^{2-}	72.08
	R.m.s deviations	
	Bond lengths/Å	0.011
	Bond angles/(°)	1.173
	Ramachandran plot (%)	
	Most Favorable	93.8
	Allowed	6.2
	Outliers	0

Values in parentheses are for highest-resolution shell. [a] $R_{work} = \Sigma_{hkl}$ |Fo(hkl) − Fc(hkl)|/Σ_{hkl} Fo(hkl). [b] R_{free} was calculated for a test set of reflections (5%) omitted from the refinement.

2 Results

2.1 Biochemical property of stDltD

PSIPRED server 4.0v indicated that stDltD from *S. thermophilus* contains a N-terminal transmembrane region from residue 7−27 aa; this finding is in accordance with that of previous reports showing DltD is a single-pass membrane protein containing a main extracellular domain[23] (Figure 1a). However, the function of the main extracellular domain is unclear. The overexpression and purification of the stDltD extracellular fragment, including residues 27−422 aa, was tested to understand how stDltD is involved in DltA/B/C/D transmembrane catalysis. The working temperature of stDltD was high because it was from the *S. thermophilus* strain. Unexpectedly, during expression, nearly no protein yielded when induction was performed at 37℃ for 5 h. stDltD performed high yield only at low temperature, such as 18℃ . A similar property was found during purification, as stDltD precipitated even under room temperature. Thus, every procedure needed to be conducted on ice. Further, Thermofluor assay confirmed that the melting temperature of stDltD was 32° C (Figure 1b), much slower than that of most proteins (over 40℃). In addition, stDltD crystallized in the space group $P2_12_12_1$ with four molecules in the asymmetric unit sharing high similarity and several contacts. SEC (Figure 1c) and AUC analysis (Figure 1d) showed that monomer is the functional unit of stDltD.

2.2 Overall structure of stDltD

The extracellular domain of stDltD consists of 23 α-helices and 5 β-strands. The 5 β-strands, β1 (66−70 aa), β2 (95−99 aa), β3 (124−129 aa), β4 (314−319 aa) and β5 (356−358 aa) are parallel to each other and inserted the helices α3 (52−60 aa) and α4 (73−76 aa), α5 (83−90 aa) and α6 (106−115 aa), α7 (117−120 aa) and α8 (131−133 aa), α18 (296−311 aa) and α19 (324−330 aa), α20 (334−351 aa) and α21 (378−392 aa), respectively (Figure 2a). This 5 β-strands situate in the center of the whole structure flanked by asymmetric helical bundles with continuous extra bundles covering on helices α1, α2, α3, α5, α6 and α16. Besides, in our stDltD structure, a typical α/β/α fold internal core was identified comprising two split regions from residue 27−139 aa and 292−422 aa which characterized by the five-stranded parallel

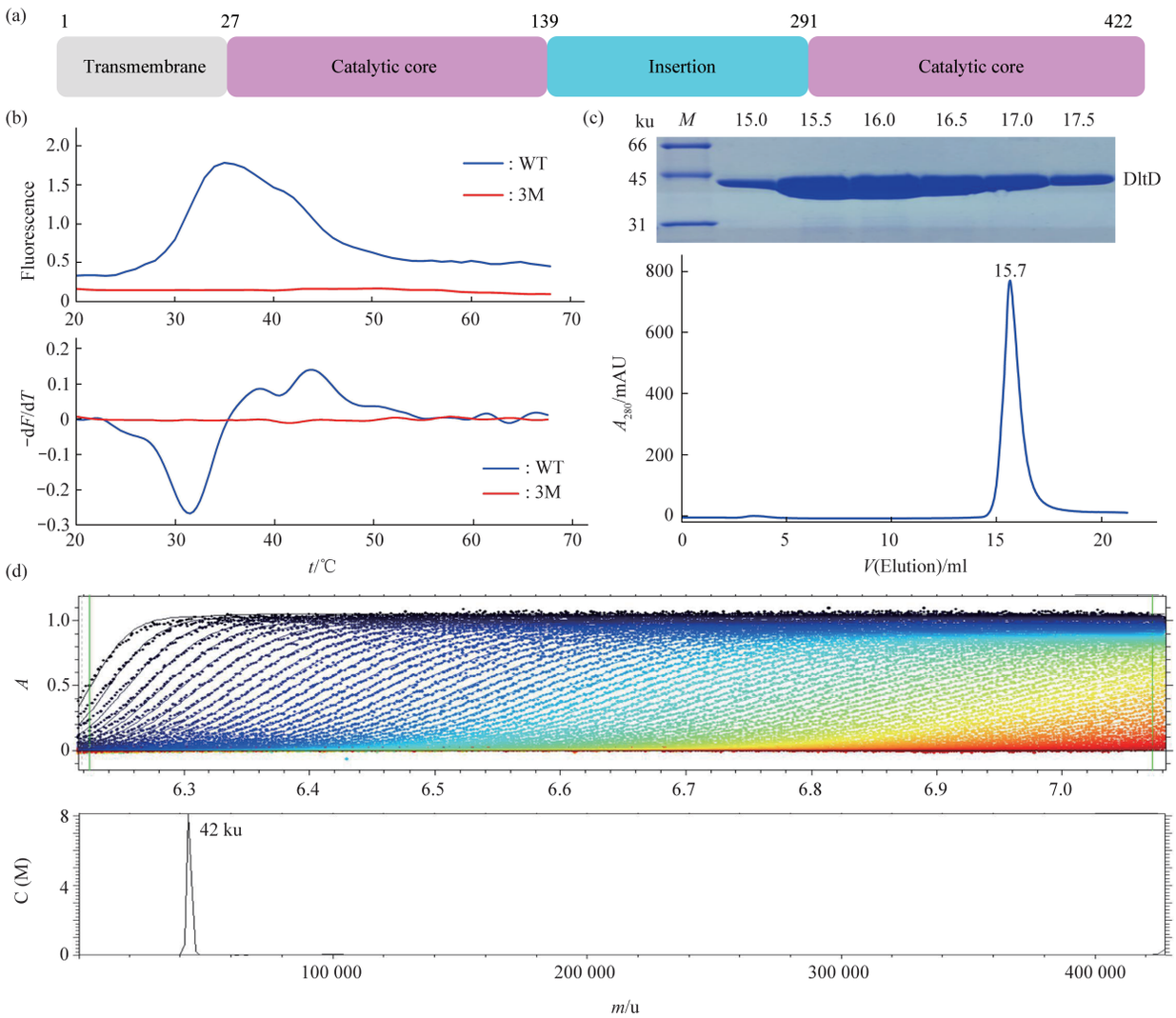

Fig. 1　Biochemical property of stDltD

(a) Schematic representation of stDltD. (b) Thermofluor assays reveal a low *T*m for WT stDltD (32℃) and undetectable for triad 3M (S73A/D371A/D374A). The upper panel shows the fluorescence change corresponding to temperature. The lower panel is the calculation of melting temperatures. (c) SEC and SDS-PAGE of stDltD and the elution peak is 15.7 ml. (d) Analytical ultracentrifugation analysis of stDltD. The upper panel shows raw sedimentation profiles of absorbance at 280 nm versus cell radius. The lower panel is the continuous sedimentation coefficient distribution.

β-sheets and flanking helical bundles (α4−α8, α18 and α20). Notably, besides the internal core, an additional insertion is formed by nine helices (α9− α17) from residue 140 to 291 aa caps around the core structure like the edge of plate.

Comparison with all other structures in the Protein Data Bank by using DALI server (http://ekhidna2. biocenter. helsinki. fi/dali/) revealed that stDltD belongs to SGNH-like family. The top three structures by DALI search were isoamyl acetate-hydrolyzing esterase (IAH1, PDB: 3MIL, *Z*=10.4, RMSD=3.2, 10% sequence identity), platelet-activating factor acetylhydrolase (gVIII-PLA2, PDB: 3DT6, *Z*=10.1, RMSD=3.0, 10% sequence identity), and lysophospholipase A (TesA, PDB: 4JGG, *Z*=9.5, RMSD=3.2, 15% sequence identity). They all belong to SGNH-like family, which includes a wide range of multifunctional proteins, such as hydrolase, thioesterase, acyltransferase, lipase, and esterases, with broad substrate specificity. Despite the low

sequence similarity, when the three structures were superimposed with stDltD, the central parallel β-sheet, the flanking helices, the catalytic triad and four conserved blocks (I, II, III and V) showed high topological conservation (Figure 2b, c). In stDltD, the strictly conserved Gly and Ser were identified in block I, while the variables Asp and Leu were substituted by Ser and Glu. In canonical α/β hydrolase, block I is usually situated in the middle region, but SGNH-like proteins showed an α/β/α sandwich-like fold with a distinct GDSL motif in block I near the N-terminus. Overall, all these structure features indicated that stDltD is a SGNH-like protein containing an SGNH-like core and a novel insertion, which may contribute to its biological function.

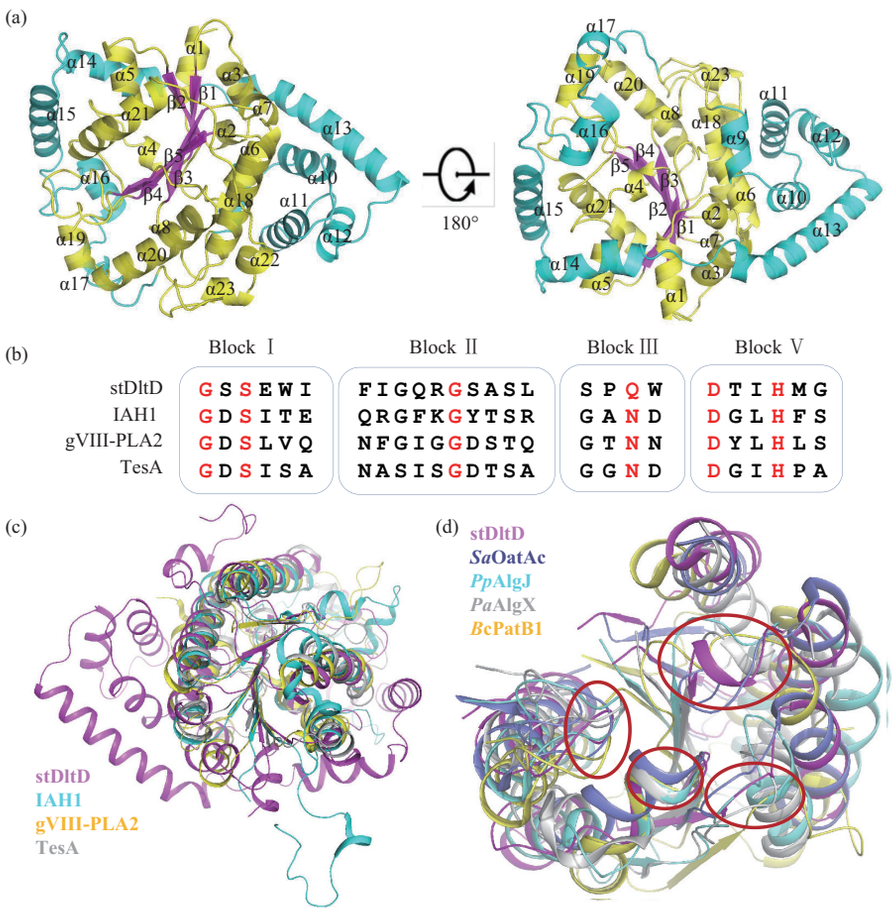

Fig. 2　Overall structure of stDltD and structure comparisons

(a) Cartoon representation of stDltD with secondary structural elements labeled (α: α-helix; β: β-strand); catalytic core is shown as yellow, insertion is cyan, five β-strands is magenta. (b) Amino acid sequence alignment of the four consensus blocks shared by members of the SGNH-like hydrolases. Red lettering denotes invariant residues. (c) Superimpositions of stDltD (in magenta) and three SGNH-like hydrolases IAH1(in cyan), gVIII-PLA (in yellow), TesA (in gray). (d) Superimpositions of stDltD (in magenta) and four acyltransfer proteins *Sa*OatAc (in blue), *Pp*AlgJ (in Cyan), *Pa*AlgX (in gray), *Bc*PatB1 (in yellow). Four typical blocks are indicated by red circle.

2.3　Comparison of transmembrane acyl modification proteins in SGNH−like family

Besides the SGNH hydrolases, stDltD showed structural similarity with other SGNH-like counterparts in transmembrane acyl modification, including AlgJ (PDB: 4O8V), AlgX (PDB: 4KNC), PatB (PDB: 5V8E) and the C-terminal domain of OatA (PDB: 6VJP), as shown in Figure 2d. They are

all terminal acyltransfer proteins coupled with MBOAT proteins for acyl modification to extracellular polymers. AlgJ and AlgX were involved in exopolysaccharide alginate acetylation in *P. aeruginosa*, and they exhibited acetylesterase activity *in vitro*[24-25]. PatB is responsible for peptidoglycan acetylation in *N. gonorrhoeae*, and enzymatic evidence of PatB1 as an O-acetyltransferase could be found[26]. Bimodular OatA comprises an N-terminal integral membrane domain and a C-terminal catalytic domain, and it serves as an acetyltransferase for peptidoglycan O-acetylation in Gram-positive bacteria[27]. In addition to sharing the αβα sandwich-like fold, stDltD shares similar catalytic features, including a catalytic triad (Ser-Asp-His) and an oxyanion hole (Gly-Asn) in four conserved blocks (Figure 2d). All these structure commonalities strongly suggested that stDltD is probably a terminal acyltransferase.

2.4 Conservational analysis of stDltD in pathogenic strains

Seven Gram-positive species, including the pathogenic strains such as *S. pneumoniae* (pneumonia), *B. anthracis* (anthrax) and *C. botulinum* (lethal toxin), were aligned using ClustalX to tackle the evolutionary conservation of stDltD. The seven species share comparable numbers of amino acids, in which the N-terminal transmembrane region and the C-terminus showed the least conservation (Figure 3). The split SGNH-like core and additional insertion generally existed in all eight species, in which four catalytic-related residues Ser, Gly, Asp, and His, along with the typical GSSE motif, were highly conserved in the corresponding blocks. The additional insertion was still widely retained in these species despite the lessened sequence conservation. These findings strongly suggested that the substrate may associated with highly conserved regions, and the additional insertion may possibly contribute to structure stability or substrate-related regulation.

2.5 Catalytic center of stDltD

StDltD contains all conserved structural elements in the SGNH family. Four conserved catalytic residues Ser73, Gly103, Asp371, and His374 existed in four conserved blocks (I, II, III, and V), respectively. Block I (71−76 aa), block II (98−107 aa), block III (130−133 aa), and block V (371−376 aa) were also spotted in the SGNH-like core (Figure 4a). In blocks I and V, Ser73, Asp371, and His374 formed a typical catalytic triad, and they were distant in sequence but spatially close enough for nucleophilic attack. In block II, Gly103 defined the typical oxyanion hole. In block III, Asn was substituted by Gln132 and Trp133 and in line closely in the similar position (Figure 4a).

The possible binding substrate of stDltD was GroP, which is the basic unit for the most pervasive LTA backbone. Through superimposed with the structure of the SGNH-like hydrolases IAH1, the glycerol molecule sit at the oxyanion hole and one hydroxyl group fit closely to the SO_4^{2-} in stDltD. On the basis of these findings, a structure model of stDltD with a GroP molecule was constructed in the catalytic pocket. The PO_4^{3-} group fit closely to Ser for nucleophile attacks, and glycerol moiety sit at the oxyanion hole. Comparison of the specific position of catalytic triad and oxyanion hole showed that the Asp371 in stDltD was situated in a loop closer to His374 and Ser73. Gln132, which is Asn83 in IAH1, was orientated 61.7° away from catalytic serine. These differences in catalytic triad and oxyanion hole may yield different efficiencies for serine nucleophile attacks (Figure 4b). Furthermore, the triad 3M (S73A/D371A/D374A) could be purified with a very low yield, and it was thermodynamically less stable (*T*m: no) than WT stDltD (*T*m = 32℃). Evidence proved that triad mutations significantly reduce the amount of D-Ala-LTA *in vivo* and *in vitro* vesicles, which was consistent with the structural importance of catalytic triad in the present study[28]. Notably, electrostatic potential revealed that the surface had bias positive and negative electrostatic patches; in particular, the catalytic site well formed a strong positively charged groove docking with a GroP molecule (Figure 4c). However, the interaction between stDltD and GroP or other small molecule analogues was not observed, indicating a more complex working scheme in physiological context.

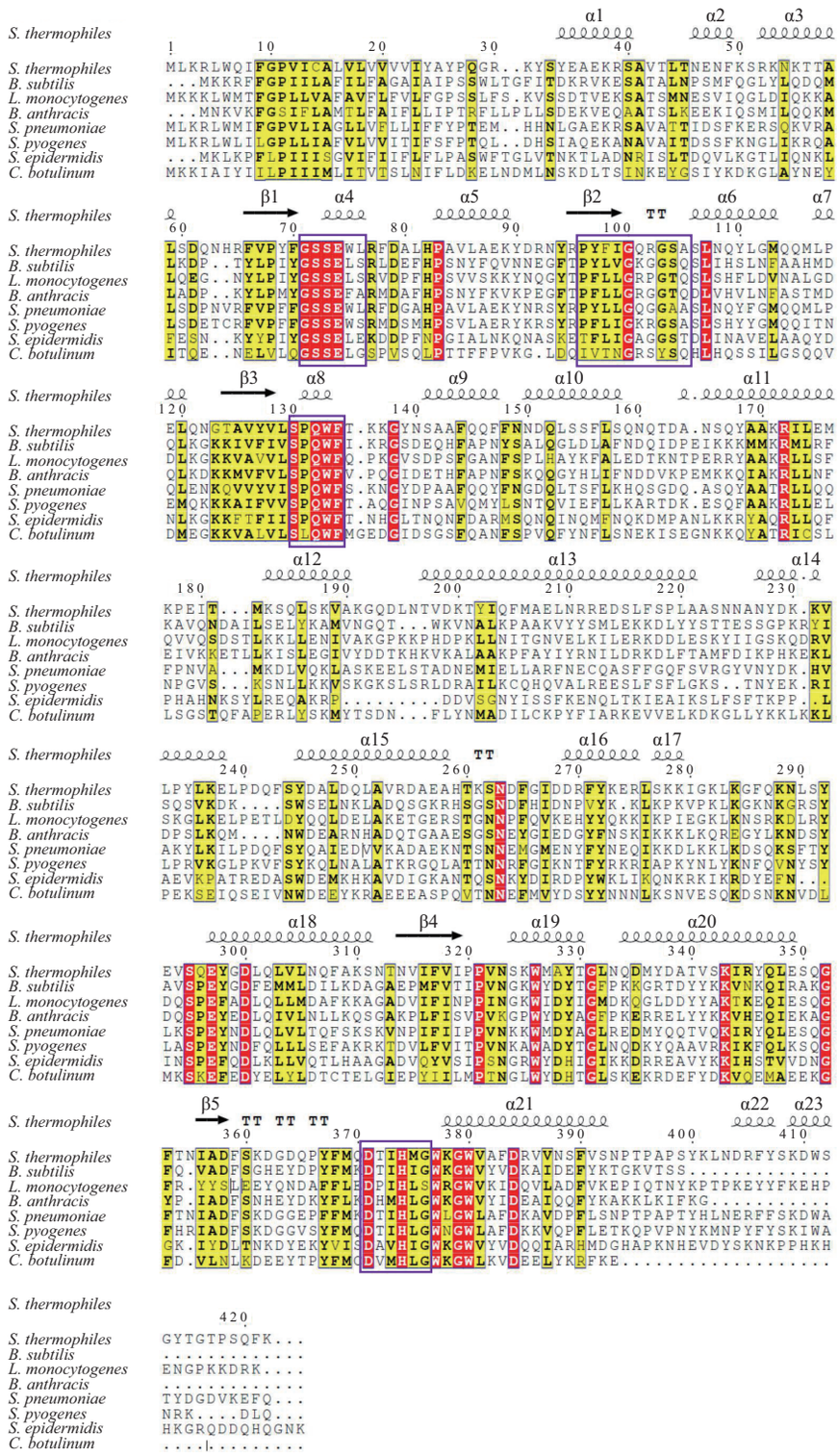

Fig. 3　Sequence alignment of stDltD in pathogenic strains

Sequence alignment was performed with ClustalX. Structure information is from stDltD, strictly conserved amino acids and similar amino acids are marked by red and yellow box, respectively. The conserved blocks are indicated by purple box. The figure was produced by ESPript.

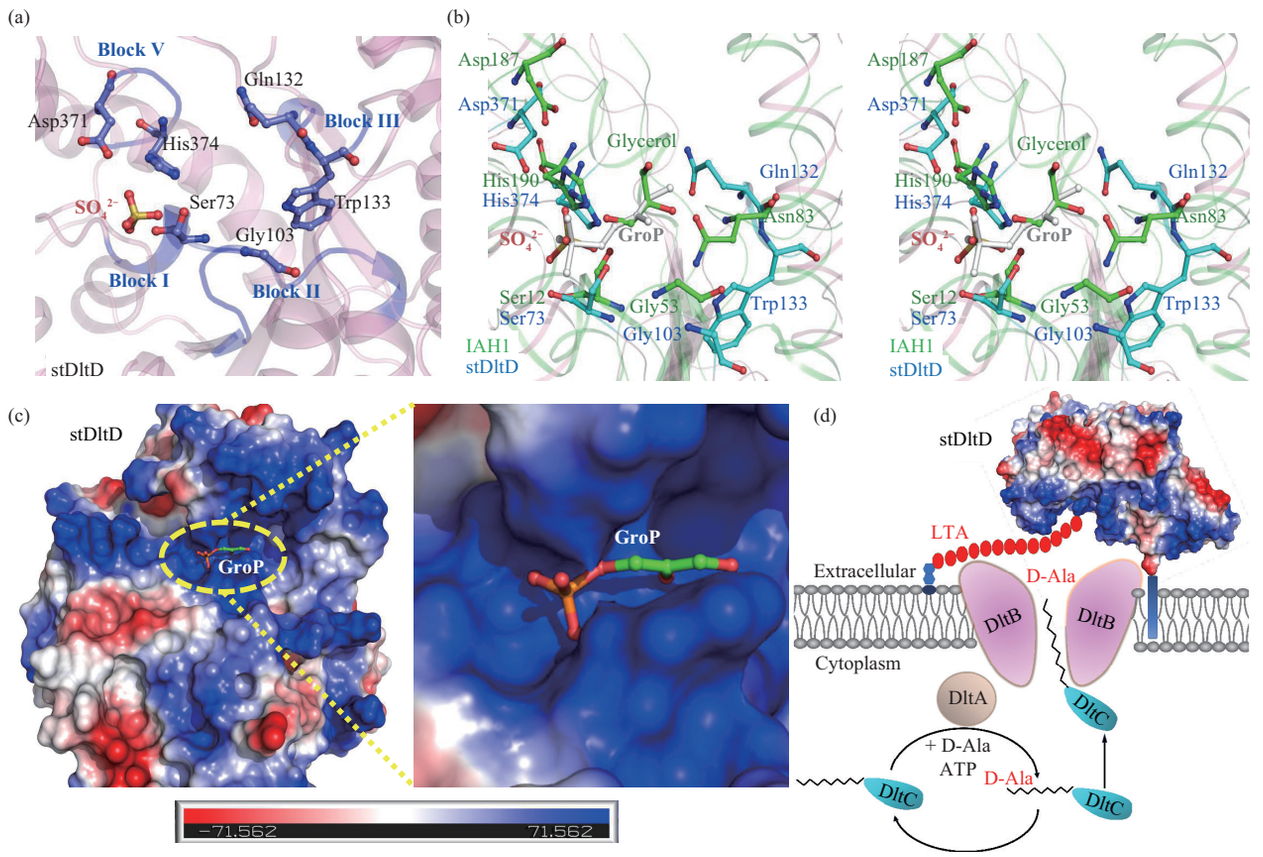

Fig. 4　Active site structure of stDltD and proposed model

(a) Active site structure of stDltD. Key residues in four conserved blocks are shown in sticks. (b) Structural superposition of catalytic centers of stDltD (in cyan) and IAH1(in green), shown in stereo. The site of SO_4^{2-} in stDltD and glycerol in IAH1 superpose well with a docking GroP molecule in active site. (c) Electrostatic potential surface map of stDltD with the same orientation as the structure in (b) shows a GroP molecule binding well in the positively charged tunnel. (d) Proposed model of dlt operon-mediated D-alanylation.

3　Discussion

Previous functional studies provided numerous evidence that DltA/B/C/D is essential for LTA and WTA D-alanine incorporation and possible transfer from first alanyled LTA to more exposed WTA. Insertional inactivation of single Dlt gene displayed a complete loss of D-alanine modifications on LTA and WTA but remained comparable amounts of glucose and GlcNAc[29]. Similar results were obtained by measuring D-^{14}C-alanine incorporation to the membrane; however, a half amount of D-alanine remained in DltD mutant[30]. A recent report showed that each deletion mutant of DltA−D became non-viable in synthetic lethal assay, and it was further confirmed by D-^{14}C-alanine detection from extracted LTA[28]. Interestingly, the poorly defined DltD was evaluated as indispensable for the final step modification. Single DltD deletion presented similar phenotypes as dlt-mutants, including defects in septum formation, increasing autolysis[31], inability for host cell adhesion and invasion[32], impaired virulence of pathogens, and susceptibility to cationic antimicrobial peptides[33]. The molecular mechanism of how DltD is served in this modification is largely unknown.

On the basis of stDltD structure, a working model for cross-membrane D-alanylation mediated by dlt operon was proposed (Figure 4d). First, cytoplasmic DltA transfers D-alanine to the Ppant moiety of DltC by using ATP to generate high-energy intermediates. D-alanyl-DltC thus serves as D-alanyl donor to form a stable complex with membrane-associated DltB sitting at the cytoplasmic bottom tunnel of DltB, where the D-Ala-Ppant group could be

coordinated properly through the membrane. The extracellular domain of stDltD is spatially close to DltB, especially the triad hole facing the funnel. Meanwhile, the LTA polymer could be caught by stDltD through electropositive groove, thus driving the cross-membrane catalysis for LTA D-alanylation. In summary, the structure provides more molecular implications to functionally characterize stDltD and cross-membrane D-alanylation, but the specific catalysis mechanism and substrate binding feature deserve further studies.

Acknowledgement We thank the staff of the beamlines BL19U1 and BL17U at Shanghai Synchrotron Radiation Facility for assistance during data collection. We also thank WILEY-VCH for the proof reading, and YANG Zhen-Wei and YU Xiao-Xia for help with Thermofluor assay and AUC analyses at Proteinscience research platform of Institute of Biophysics.

References

[1] Auer G K, Weibel D B. Bacterial cell mechanics. Biochemistry, 2017, **56**(29): 3710-3724

[2] Rajagopal M, Walker S. Envelope structures of gram-positive bacteria. Curr Top Microbiol Immunol, 2015, **404**(1): 1-44

[3] Silhavy T J, Kahne D, Walker S. The bacterial cell envelope. Cold Spring Harb Perspect Biol, 2010, **2**(5): 414-424

[4] Strahl H, Errington J. Bacterial membranes: structure, domains, and function. Annu Rev Microbiol, 2017, **71**(8): 519-538

[5] Koch H U, Haas R, Fischer W. The role of lipoteichoic acid biosynthesis in membrane lipid metabolism of growing *Staphylococcus aureus*. Eur J Biochem, 1984, **138**(2): 357-363

[6] Kojima N, Araki Y, Ito E. Structure of the linkage units between ribitol teichoic acids and peptidoglycan. J Bacteriol, 1985, **161**(1): 299-306

[7] Brown S, Santa Maria J P J, Walker S. Wall teichoic acids of gram-positive bacteria. Annu Rev Microbiol, 2013, **67**(1): 313-336

[8] Percy M G, Grundling A. Lipoteichoic acid synthesis and function in gram-positive bacteria. Annu Rev Microbiol, 2014, **68**(1): 81-100

[9] Neuhaus F C, Baddiley J. A continuum of anionic charge: structures and functions of D-alanyl-teichoic acids in gram-positive bacteria. Microbiol Mol Biol Rev, 2003, **67**(4): 686-723

[10] Xia G, Kohler T, Peschel A. The wall teichoic acid and lipoteichoic acid polymers of *Staphylococcus aureus*. Int J Med Microbiol, 2010, **300**(2): 148-154

[11] Damjanovic M, Kharat A S, Eberhardt A, *et al*. The essential tacF gene is responsible for the choline-dependent growth phenotype of *Streptococcus pneumoniae*. J Bacteriol, 2007, **189**(19): 7105-7111

[12] Morath S, Geyer A, Hartung T. Structure-function relationship of cytokine induction by lipoteichoic acid from *Staphylococcus aureus*. J Exp Med, 2001, **193**(3): 393-397

[13] Iwasaki H, Shimada A, Ito E. Comparative studies of lipoteichoic acids from several *Bacillus* strains. J Bacteriol, 1986, **167**(2): 508-516

[14] Childs W C, Taron D J, Neuhaus F C. Biosynthesis of D-alanyl-lipoteichoic acid by *Lactobacillus casei*: interchain transacylation of D-alanyl ester residues. J Bacteriol, 1985, **162**(3): 1191-1195

[15] Kiriukhin M Y, Neuhaus F C. D-alanylation of lipoteichoic acid: role of the D-alanyl carrier protein in acylation. J Bacteriol, 2001, **183**(6): 2051-2058

[16] Koch H U, Doker R, Fischer W. Maintenance of D-alanine ester substitution of lipoteichoic acid by reesterification in *Staphylococcus aureus*. J Bacteriol, 1985, **164**(3): 1211-1217

[17] Hurst A, Hughes A, Duckworth M, *et al*. Loss of D-alanine during sublethal heating of *Staphylococcus aureus* S6 and magnesium binding during repair. J Gen Microbiol, 1975, **89**(8): 277-284

[18] Ma D, Wang Z, Merrikh C N, *et al*. Crystal structure of a membrane-bound O-acyltransferase. Nature, 2018, **562**(7726): 286-290

[19] Otwinowski Z, Minor W. Processing of X-ray diffraction data collected in oscillation mode. Methods Enzymol, 1997, **276**(1): 307-326

[20] Winn M D, Ballard C C, Cowtan K D*et al*. Overview of the CCP4 suite and current developments. Acta Crystallogr D Biol Crystallogr. 2011, **67**(4): 235-242

[21] Adams P D, Afonine P V, Bunkóczi G, *et al*. PHENIX: a comprehensive Python-based system for macromolecular structure solution. Acta Crystallogr D Biol Crystallogr, 2010, **66**(2): 213-221

[22] Emsley P, Cowtan K. Coot: model-building tools for molecular graphics. Acta Crystallogr D Biol Crystallogr, 2004, **60**(12): 2126-2132

[23] Reichmann N T, Cassona C P, Grundling A. Revised mechanism of D-alanine incorporation into cell wall polymers in gram-positive bacteria. Microbiology, 2013, **159**(9): 1868-1877

[24] Riley L M, Weadge J T, Baker P, *et al*. Structural and functional characterization of *Pseudomonas aeruginosa* AlgX: role of AlgX in alginate acetylation. J Biol Chem, 2013, **288**(31): 22299-22314

[25] Baker P, Ricer T, Moynihan P J, *et al*. *P. aeruginosa* SGNH hydrolase-like proteins AlgJ and AlgX have similar topology but separate and distinct roles in alginate acetylation. PLoS Pathog, 2014, **10**(8): 4334-4340

[26] Sychantha D, Little D J, Chapman R N, *et al*. PatB1 is an O-acetyltransferase that decorates secondary cell wall polysaccharides. Nat Chem Biol, 2018, **14**(1): 79-85

[27] Jones C S, Sychantha D, Howell P L, *et al*. Structural basis for the O-acetyltransferase function of the extracytoplasmic domain of OatA from *Staphylococcus aureus*. J Biol Chem, 2020, **295**(24): 8204-8213

[28] Wood B M, Santa Maria J P J, Matano L M, *et al*. A partial

reconstitution implicates DltD in catalyzing lipoteichoic acid D-alanylation. J Biol Chem, 2018, **293**(46):17985-17996

[29] Perego M, Glaser P, Minutello A, *et al*. Incorporation of D-alanine into lipoteichoic acid and wall teichoic acid in *Bacillus subtilis*. Identification of genes and regulation. J Biol Chem, 1995, **270**(26): 15598-15606

[30] Debabov D V, Kiriukhin M Y, Neuhaus F C. Biosynthesis of lipoteichoic acid in *Lactobacillus rhamnosus*: role of DltD in D-alanylation. J Bacteriol, 2000, **182**(10): 2855-2864

[31] Perea Velez M, Verhoeven T L, Draing C, *et al*. Functional analysis of D-alanylation of lipoteichoic acid in the probiotic strain *Lactobacillus rhamnosus* GG. Appl Environ Microbiol, 2007, **73**(11): 3595-3604

[32] Steen A, Palumbo E, Deghorain M, *et al*. Autolysis of *Lactococcus lactis* is increased upon D-alanine depletion of peptidoglycan and lipoteichoic acids. J Bacteriol, 2005, **187**(1): 114-124

[33] Henneke P, Morath S, Uematsu S, *et al*. Role of lipoteichoic acid in the phagocyte response to group B *Streptococcus*. J Immunol, 2005, **174**(10): 6449-6455

嗜热链球菌dlt操纵子终端亚基stDltD的晶体结构*

曾　琪[1,2]　田利飞[1]　刘晏平[1]　闫小雪[1)**]　许文青[1,3)**]

（[1)] 中国科学院生物物理研究所，中国科学院生物大分子研究中心，生物大分子国家重点实验室，北京 100101；
[2)] 中国科学院大学生命科学学院，北京 100049；[3)] 上海科技大学生命科学与技术学院，上海高级免疫化学研究所，上海 201210）

摘要　细胞表面多聚物的酰基跨膜修饰对增强细菌的致病性至关重要. DltA/B/C/D操纵子介导的脂磷壁酸（LTA）D-丙酰化修饰是革兰氏阳性菌中重要的一类后修饰，其调节膜内外的电荷平衡. DltA/B/C/D操纵子主要由DltA、DltB、DltC 和DltD四种蛋白质亚基组成，其催化机制与结构在生物进化中高度保守. DltA/DltC介导的胞内D-丙酰胺的转移机理已有深入的研究，而跨膜O-酰基转移酶DltB和dlt操纵子末端DltD介导的跨膜催化过程并不清楚. 本文解析了来源于嗜热链球菌（*S. thermophilus*）中stDltD膜外结构域2.94 Å分辨率的晶体三维结构. 结构比对分析表明，stDltD是dlt操纵子终端的酰基转移酶，属于SGNH-like家族，stDltD的活性中心，包括4个blocks和催化三联体，都保守存在于多种革兰氏阳性病原菌中. 此外，结构叠合分析表明，stDltD催化中心形成的正电荷窝沟正好可以结合一个脂磷壁酸骨架的单体即甘油磷酸分子. 在前人的研究基础上，我们提出了一个由Dlt/A/B/C/D操纵子介导跨膜D-丙酰化修饰的工作模型. 本研究对进一步阐明DltD的生物学功能以及Dlt/A/B/C/D操纵子酰基跨膜修饰的分子机制具有重要意义.

关键词　dlt操纵子，酰基跨膜修饰，LTA D-丙酰化修饰，SGNH-like蛋白家族，晶体结构
中图分类号　Q5，Q6　　**DOI**：10.16476/j.pibb.2021.0020

* 中国科学院先导B专项（XDB37030302）、国家自然科学基金（31629002）和大分子国家重点实验室开放课题资助项目.
** 通讯联系人.
闫小雪. Tel：010-64888509，E-mail：snow@ibp.ac.cn
许文青. Tel：010-64888509，E-mail：xuwq2@shanghaitech.edu.cn
收稿日期：2021-01-19，接受日期：2021-03-01